ARCHIVES of FOUNDRY ENGINEERING
Published quarterly as the organ of the Foundry Commission of the Polish Academy of Sciences
ISSN (1897-3310)
Volume 14
Special Issue
1/2014
121-126
24/1

Temperature Field in Surfaced Steel Casts with the Heat of the Weld Taken into Account

J. Winczek[a*]
[a]The Faculty of Mechanical Engineering and Computer Science, Czestochowa University of Technology
Armii Krajowej 21, 42-201 Czestochowa, Poland
[*]Corresponding author: E-mail address: winczek@imipkm.pcz.czest.pl

Received 03.03.2014; accepted in revised form 31.03.2014

Abstract

In this work a model of temperature field in a steel cast during surfacing was presented. Analytical solution for half-infinite body model was obtained by aggregating temperature increments caused by applying liquid metal and heat radiation of moving electrode. The assumptions were Gaussian distribution heat sources of applied metal and weld and of electric arc heat source. Computations of temperature field were carried out during surfacing of cuboidal steel cast. The results were presented as temporary and maximum temperature distribution in element's cross section and thermal cycles at selected points. The accuracy of solution was verified comparing calculated fusion line to that obtained experimentally.

Słowa kluczowe: Surface Treatment, Temperature Field, Welding, Surfacing

1. Introduction

Welding techniques are often used to regenerate or improve the quality of the casting surface. In this area, intense experimental research on the surfacing by welding [1-5] and surface melting [6-9] is caried out, as well as the thermal measurements of bonding processes [10,11]. Attempts are also made at modeling of thermo-mechanical phenomena occurring in these processes.

The basis for welding processes processing is the usage of concentrated moving heat source, which causes temperature field changeable in time and space. Two approaches dominate during these processes of modeling temperature field. The first one – numerical, in which the finite difference methods, infinitesimal heat balances and FEM are used [12-20]. The second approach consists of analytical solution, described further in this work, where integral transformations and Green's function method are used most frequently.

Rosenthal's [21, 22] and Rykalin [23, 24] works initiated the modeling of temperature field developed by the moving heat source. Rosenthal was the first to obtain temperature distribution equation for quasistationary state for various heat source models (point, linear, and surface) by introduction of thermo-mechanical properties of heated material independent on temperature. Rosenthal assumed the heat source in the form of segment parallel to the weld axis, while Rykalin in the form of perpendicular segment.

Relying on Rosenthal's solutions to the point heat source Christensen et al. [25] proposed no-dimensional solutions to temperature field which enable to define measurements of the heat affected zone and speed of cooling. Eagar and Tsai [26] modified Rosenthal's model including 2D Gaussian distributed heat source and developed solution to travelling heat source in a semi-infinite steel plate.

The model of double ellipsoidal three-dimensional heat source was first introduced by Goldak et al. [27]. The finite elements method was used to determine temperature field in sheet weld. Bo and Cho [28] derived analytical solution for transient temperature field in finite thickness plate during single pass arc welding. The

heat source due to electric arc was assumed to take traveling Gaussian distribution, likewise as Eagar and Tsai.

The analytical solution to temperature field of fillet weld was presented by Jeong and Cho [29] for infinite plate of finite thickness bent at right angle. Analytical 3-D model of temperature field in halfinfinite body caused by 3-D moving heat source was formulated by Ngyen et al. [30] and experimentally tested by measurement of temporary temperature in various point of bead at the plate and in the middle of weld pool. In solution has been used double ellipsoidal heat source proposed by Goldak et al. [27].

Fassani and Trevisan [31] compared thermal cycles during multi-pass GMAW welding calculated for Rosenthal's point heat source models and one-dimensional of Gaussian distribution. Analytical solution was presented for one-dimensional issue – distribution of temperature perpendicular to the direction of welding.

Nguyen et al. [32] presented analytically approximated solution for single and double ellipsoidal heat source model in modeling of temperature field of finite thickness. Authors proposed also solution to ellipsoidal heat source in dimensional form.

The analytical solution to heat conduction equation offers quick assessment of temperature field and its dependence on parameters such as e.g., heat source velocity and its power. In most cases of temperature field solution, thus far as a heat source was used the energy of electric arc.

Kang and Cho [33] solved temperature field in welding model using GTA method taking into consideration filler wire. Surfacing by welding is distinguished by applying liquid metal, which spills across the surface and constitutes additional heat source. The necessity of taking into consideration the heat of melted metal in temperature field solutions in welding processes is therefore essential.

2. Analytical description of temperature field during surfacing

Single-distributed heat source models accepted in the descriptions of the temperature field during surfacing by welding, do not allow for restoration of irregular isotherms shapes (including the fusion line), therefore a bimodal model is proposed, finding justification in the way of transmitting heat generated by an electric arc to the surfaced object. As a temperature field solution is proposed the aggregation of temperature fields caused by action of applied bead and electric arc:

$$T(x,y,z,t)-T_0=\sum_{i=1}^{2}\Delta T_i \tag{1}$$

where ΔT_1 and ΔT_2 are temperature accruals caused by the heat of liquid metal of weld and electric arc respectively.

The analytical description of the mentioned above field is obtained using the heat conduction equation in fixed Cartesians coordinate system (x, y, z):

$$\nabla(\lambda\nabla T)+q=c\rho\frac{\partial T}{\partial t} \tag{2}$$

where c – specific heat [J/kg K], ρ - density [kg/m^3], λ - coefficient of heat conduction [W/m K], T – temperature, t – time, which for infinite body with temporary heat source q [J] applied at optional point of body with coordinates (x', y', z') takes the following form [34, 35]:

$$T(x,y,z,t)= =\frac{q}{c\rho(4\pi at)^{3/2}}\exp\left(-\frac{(x-x')^2+(y-y')^2+(z-z')^2}{4at}\right) \tag{3}$$

where a – thermal diffusivity [m^2/s].

Based on this solution for point source and solutions for planar [36] and volumetric [37, 38] sources, temperature at point P with coordinates (x, y, z) ξ meters away from source (Fig. 1) can be desribed by:

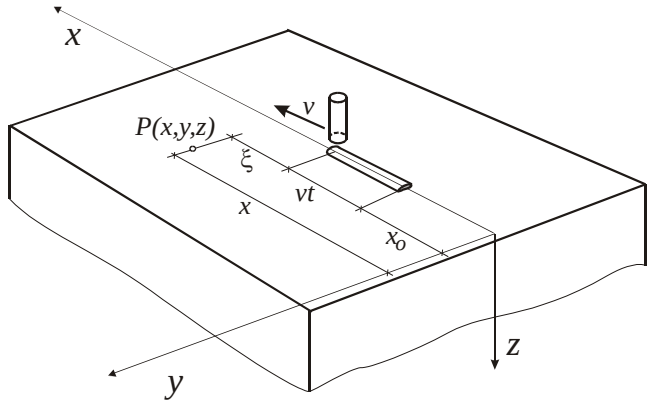

Fig. 1. The scheme of single-pass surfacing

- for time $t \le t_c$, where t_c means total time of making weld:

$$\Delta T_i = A_i^H\int_0^t F_i^H(t'')dt'' \tag{4}$$

- for time $t > t_c$:

$$\Delta T_i = A_i^C\int_0^{t_c} F_i^C(t')dt' \tag{5}$$

where

$$A_i^H=\frac{3}{8}\frac{\dot{q}_i}{c\rho\pi az_{0i}}\exp\left(-\frac{v\xi}{2a}-\frac{v^2t_{0i}}{4a}\right) \tag{6}$$

$$A_i^C = \frac{3}{8}\frac{\dot{q}_i}{c\rho\pi a z_{0i}} \tag{7}$$

$$F_H(t'') = \frac{1}{t''+t_{0i}}\exp\left(-\frac{\xi^2}{4a(t''+t_{0i})}-\frac{v^2 t''}{4a}\right)$$
$$\left(\left(1-\frac{z^2+2at'')}{z_{0i}^2}\right)\left(erf\left(\frac{z+z_{0i}}{2(at'')^{0,5}}+\right.\right.$$
$$-\Phi(z)erf\left(\Phi(z)\frac{z-z_{0i}}{2(at'')^{0,5}}\right)\Bigg)+ \tag{8}$$
$$\frac{4at''}{z_{0i}^2}\left(\frac{z+z_{0i}}{(4\pi at'')^{0,5}}\exp\left(-\frac{(z-z_{0i})^2}{4at''}\right)+\right.$$
$$\left.-\frac{z-z_{0i}}{(4\pi at'')^{0,5}}\exp\left(-\frac{(z+z_{0i})^2}{4at''}\right)\right)$$

$$F_C(t') = \frac{1}{t+t_{0i}-t'}$$
$$\exp\left(-\frac{(x-v\,t'-x_0)^2+(y-y_0)^2}{4a(t+t_{0i}-t')}\right)$$
$$\left(\left(1-\frac{z^2+2a(t-t')}{z_{0i}^2}\right)\left(erf\left(\frac{z+z_{0i}}{2(a(t-t'))^{0,5}}\right)+\right.\right. \tag{9}$$
$$-\Phi(z)erf\left(\Phi(z)\frac{z-z_{0i}}{2(a(t-t'))^{0,5}}\right)\Bigg)+$$
$$\frac{4a(t-t')}{z_{0i}^2}\left(\frac{z+z_{0i}}{(4\pi a(t-t'))^{0,5}}\exp\left(-\frac{(z-z_{0i})^2}{4a(t-t')}\right)+\right.$$
$$\left.\left.-\frac{z-z_{0i}}{(4\pi a(t-t'))^{0,5}}\exp\left(-\frac{(z+z_{0i})^2}{4a(t-t')}\right)\right)\right)$$

$$\Phi(z) = \begin{cases} -1 & for \quad z \in \langle 0, z_{0i}\rangle \\ 1 & for \quad z \in (z_{0i}, \infty) \end{cases} \tag{10}$$

$$\dot{q}_2 = \eta UI - \dot{q}_1 \tag{11}$$

$$t_c = l/v \tag{12}$$

z_0 [m] denotes depth of heat source deposition, while quantity t_{0i} [s] characterise the surface heat distribution, so that:

$$r_i^2 = 4at_{0i} \tag{13}$$

where r_i [m] denotes averaged radius of Gaussian distributed heat source [39], U [V], I [A] and η are voltage, amperage and arc efficiency respectively, l [m] length of the weld, and v [m/s] welding velocity (of electrode). Total amount of heat q_1 contained in the material of melted electrode is expressed by relationship [40]:

$$q_1 = \Delta q_{solid} + \Delta q_f + \Delta q_{liqiud} \tag{14}$$

where Δq_{solid} – heat necessary to heat-up the electrode from initial temperature to melting temperature, Δq_f – heat used for melting the electrode (heat of fusion), Δq_{liquid} – heat used for heating-up melted material to the temperature, in which the drop of metal falls on the surface of welded material. The initial temperature of electrode T_e from the welding head is set at 100 ^{0}C. On account of this we get:

$$\dot{q}_1 = \dot{m}\left(c(T_L - T_e) + L\right) \tag{15}$$

where

$$\dot{m} = \rho_e \frac{\pi d^2}{4} v_e \tag{16}$$

T_L – temperature at which metal leaves the wire tip [K], L – latent heat of fusion [J/kg], v_e [m/s] – velocity of passing electrode wire with diamater d [m] and density ρ_e [kg/m^3].

The face of a weld is determined mainly by surface tension forces. Basing on experimental researches Hrabe et al. [41] proposed the parabolic shape of the face of a weld, which has been applied in this work.

3. Example of computations

Computations of changeable in time temperature field for 230-450W steel cast in shape of side of length 0,1 m and width 0,4 m during single-pass surfacing have been conducted. Thermal properties of welded subject material and electrode have been determined by a = 8·10^{-6} m^2/s , c = 670 J/kg K, ρ = 7800 kg/m^3 ($c\rho$ = 5,2·10^6 J/K m^3) and L = 268 kJ/kg.

Numerical simulations have been conducted for voluminal sources with Gaussian distribution of power density distinguished by z_{01}= 0,005 m i t_{01} = 4,5 s oraz z_{02}= 0,005 m i t_{02} = 4,5 s. The sum of heat's powers corresponds to welding parameters (U = 24,3 V, I = 232 A, η = 0,6) used in welding trials using GMA method conducted by Klimpel et al. [42] in single-pass surfaced element from S235 steel.

Likewise in experiment, in calculations were assumed welding velocity v = 0,007 m/s, electrode wire diameter d = 1,2 mm, wire feed speed v_e = 0,013 m/s and bead dimensions h_w = 2,77 mm and w_w = 11,93 mm.

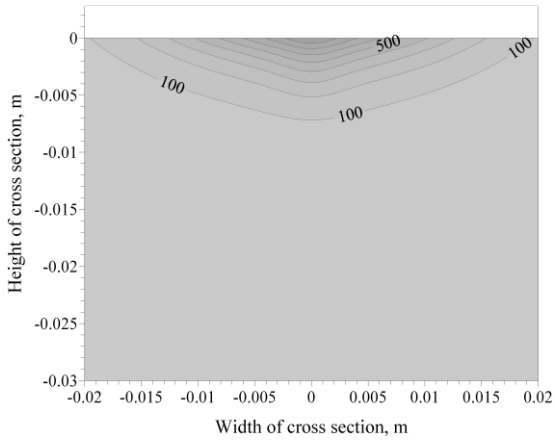

Fig. 2. Temperature field 0,5 s before the passage of electrode

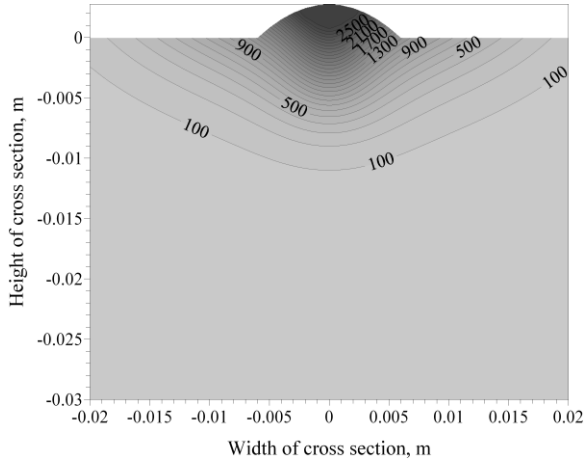

Fig. 3. Temperature field 0,5 s after the passage of electrode

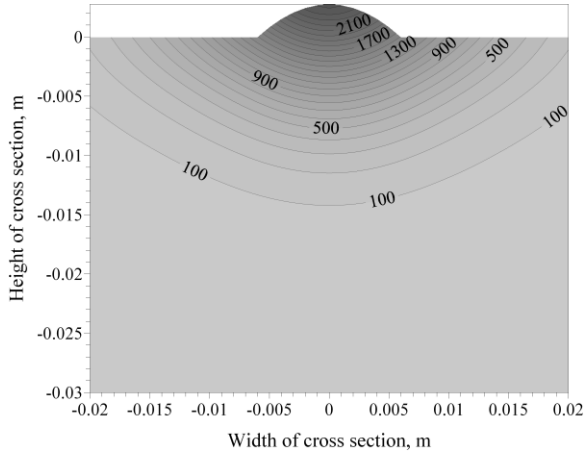

Fig.4. Temperature field 2 s after the passage of electrode

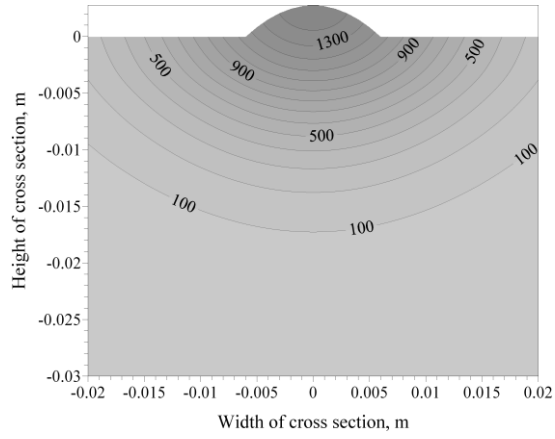

Fig. 5. Temperature field 4 s after passage of electrode

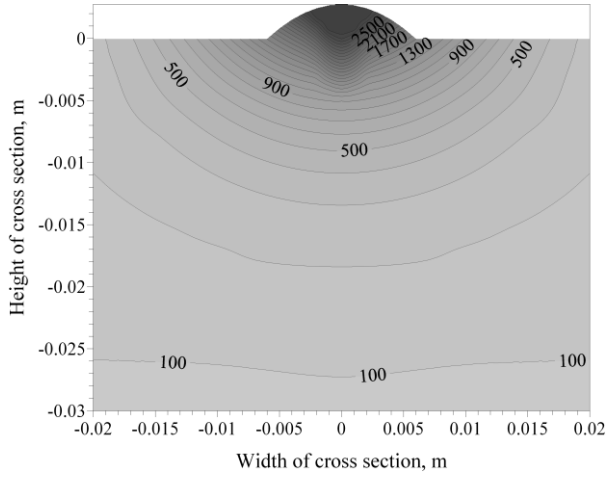

Fig. 6. Maximum temperature field

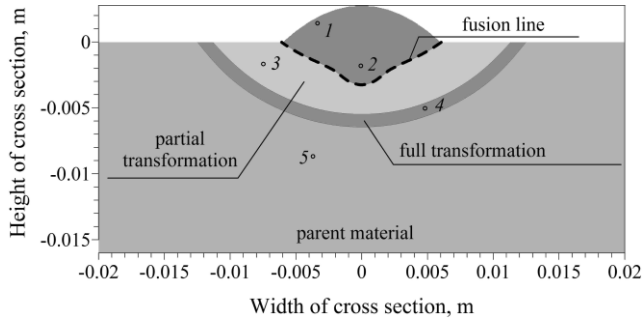

Fig. 7. Heat affected zone with selected points: dashed line – fusion line obtained experimentally [42]

Analysis of temperature field in middle cross-section of surfaced steel cast has been made. In figures 2 - 5 have been presented temperature distribution during surfacing: 0,5 s before

(Fig. 2) and 0,5 s (Fig. 3), 2 s (Fig. 4) and 4 s (Fig. 5) after passage of electrode and application of weld. Figure 6 presents maximum temperatures in cross section.

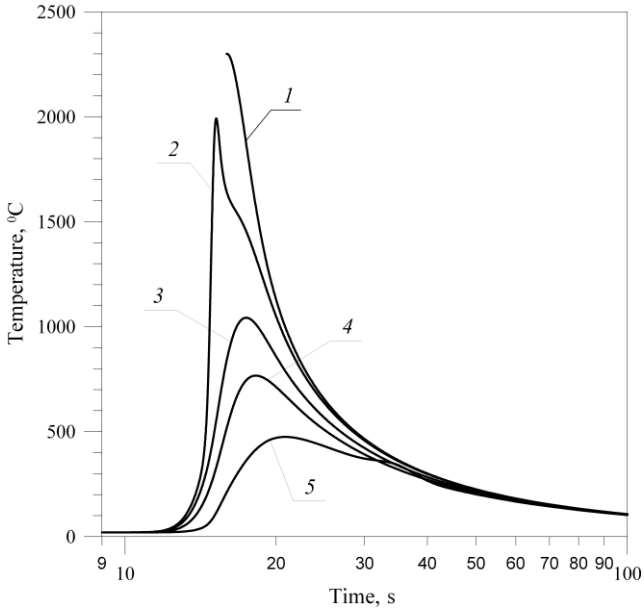

Fig. 8. Thermal cycles at selected points of cross section

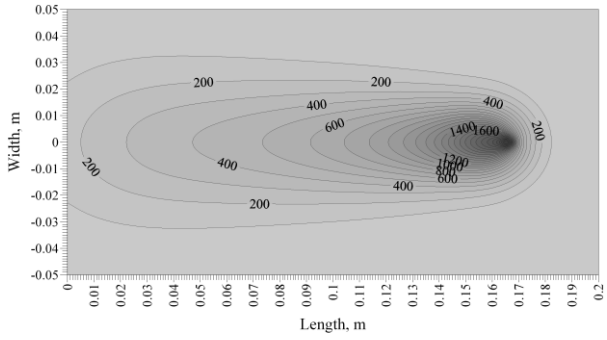

Fig. 9. Temperature isolines on the surface of surfaced steel cast after 25 s of surfacing.

Figure 7 in turn presents heat affected zones determined by the initial (A_1 =720 ^{0}C) and final (A_3 = 835 ^{0}C) temperature of austenitic transformation as well as fusion line (1493 ^{0}C). Fusion line (solidification temperature of steel) in this figure corresponds to fusion line obtained in experiment described by Klimpel et al. [42]. Thermal cycles in selected points of cross section (cf. Fig. 7) have been presented in Fig. 8. Temperature distribution on the surface of surfaced steel cast after 25 s of surfacing (10 s after passage above middle cross-section with the coordinate x = 0,1 m) is presented in Fig. 9.

4. Conclusions

Surfacing is distinguished by application of liquid metal, which spills across the surface and creates additional heat source. Consideration of this heat source is therefore essential in temperature field solutions. In work has been presented temperature field solution of surfacing for half-infinite body model. The solution was obtained by aggregation of temperature accruals caused by applying liquid metal and thermal radiation from moving electrode. The accuracy of solution was confirmed by comparison of calculated fusion line with obtained experimentally by other researchers.

Presented model enables determination of heat affected zone (HAZ), including partial and full transformations and fusion zones, as well as analysis of thermal cycles at optional point of cast steel cast.

References

[1] Adamiec J., Markusik M., Skrzypczak A. (2006). The repair of magnesium alloy castings with the help of welding techniques. *Archiv. Foundry* 6(18)(1/2) 215-220 (in Polish).

[2] Szajnar J., Wróbel P., Wróbel T. (2006). TIG - surfacing - method of repair chromium cast with castings defects. *Archiv. Foundry* 6(22) 490-496 (in Polish).

[3] Szajnar J., Stawarz M., Wróbel P., Wróbel T. (2007). Properties shaping and rep air of selected types of cast iron. *Archiv. Foundry Eng.* 7(2) 87-90.

[4] Szajnar J., Wróbel P., Wróbel T. (2008). Application of welding technology TIG to cast iron repair. *Archiv. Foundry* 8(1) 317-320.

[5] Wojciechowski W., Kowalski J.S. (2013). Welding technology in foundry. *Archiv. Foundry* 13(1) 87-90 (in Polish).

[6] Opiekun Z.A., Trytek A. (2006). Effect of plasma gas on heat absorber by surface remelting Mar-M509 cobalt casting alloy. *Archiv. Foundry* 6(18 – 1/2) 401-406 (in Polish).

[7] Opiekun Z.A., Trytek A. Hardness and microstructure surface molten of Mar-M509 cobalt casting alloy. *Archiv. Foundry* 6(18 – 1/2) 401-406 (in Polish).

[8] Orłowicz W., Trytek A. (2006). Surface melting of cast iron alloy with chromium. *Archiv. Foundry* 6(18 – 2/2) 313-318 (in Polish).

[9] Orłowicz A., Trytek A. (2007). Development of microstructure and performance of cast iron surface enriched plasma arc. Mongraph. *Archiv. Foundry* 7(23) (in Polish).

[10] Orłowicz W., Trytek A. (2006). The thermal efficiency and melting efficiency of the audion process on cast iron with Cr. *Archiv. Foundry* 6(18 – 2/2) 319-324 (in Polish).

[11] Orłowicz W., Betleja J., Mróz M., Trytek A., Tupaj M., The flow calorimeter for heat measuring in the bonding process. Copyright invention (patent) No PL211283 granted by the Polish Patent Office.
[12] Mahapatra M.M., Datta G.L., Pradhan B (2006). Three-dimensional finite element analysis to predict the effects of shielded metal arc welding process parameters on temperature distributions and weldment zones in butt and one-sided fillet welds. *Proc. I. Mech.* 220, *J. Eng. Manuf.* 837-884.
[13] Kumar A., DebRoy T. (2007). Heat transfer and fluid flow during gas-metal-arc fillet welding for various joint configurations and welding positions. *Metall. Mater. Trans.* 38A, 506-519.
[14] Wang S., Goldak J., Zhou J., Tchernov S., Downey D. (2009). Simulation on the thermal cycle of a welding process by space-time convection-diffusion finite element analysis. *Int. J. Thermal Sci.* 48, 936-947.
[15] Deng D. (2009). FEM prediction of welding residual stress and distortion in carbon steel considering phase transformation effects. *Mater. Dsgn.* 30, 359-366.
[16] Jiang W., Liu Z., Gong J.M., Tu S.T. (2010). Numerical simulation to study the effect of repair width on residual stresses of stainless steel clad plate. *Int. J. Pres. Ves. Pip.* 87, 457 – 463.
[17] Lee H.T., Chen C.T., Wu J.L. (2010). 3D numerical study of effects of temperature field on sensitisation of Alloy 690 butt welds fabricated by gas tungsten arc welding and laser beam welding. *Sci. Technol.Weld. Join.* 15, 605-612.
[18] Piekarska W., Kubiak M., Bokota A. (2011). Numerical simulation of thermal phenomena and phase transformations in laser-arc hybrid welded joint. *Arch. Metall. Materials* 56(2), 409-421.
[19] Piekarska W., Kubiak M. (2011). Three-dimensional model for numerical analysis of thermal phenomena in laser-arc hybrid welding process, *Int. J. Heat Mass Transfer* 54, 4966-4974.
[20] Chen J., Schwenk C., Wu C.S., Rethmeier M. (2012). Predicting the influence angle on heat transfer and fluid flow for new gas metal arc processes. *Int. J. Heat Mass Transfer* 55, 102-111.
[21] Rosenthal D. (1941). Mathematical theory of heat distribution during welding and cutting. *Weld. J.* 20, 220s – 234s.
[22] Rosenthal D. (1946). The theory of moving sources of heat and applications to metal treatments. *Trans. ASME*, 11, 849 – 866.
[23] Rykalin N.N. (1947). *Thermal fundamentals of welding*. AN SSSR, Moskva (in Russian).
[24] Rykalin N.N. (1951) *Calculations of heat processes in welding*. Mašgiz, Moskva (in Russian).
[25] Christensen N., Davies V.L., Gjermundsen K. (1965). Distribution of temperatures in arc welding. *British Weld. J.* 2, 54-75.
[26] Eagar T.W., Tsai N.S. (1983). Temperature fields produced by travelling distributed heat sources. *Welding J.* 62, 346s-355s.
[27] Goldak J., Chakravarti A., Bibby M. (1985). A double ellipsoidal finite element model for welding heat source. II W Doc. No. 212-603-85.
[28] Bo K.S., Cho H.S. (1990). Transient temperature distribution in arc welding of finite thickness plates. *Proc. Inst. Mech. Eng.* B3(204), 175-183.
[29] Jeong S.K., Cho H.S. (1997). An analytical solution to predict the transient temperature distribution in fillet arc welds. *Welding J.* 76, 223s – 232s.
[30] Nguyen N.T., Matsuoka K., Suzuki N., Maeda Y. (1999). Analytical solutions for transient temperature of semi-infinite body subjected to 3-D moving heat sources. *Welding J.* 78, 265s-274s.
[31] Fassani R.N.S. (2003). Analytical modeling of multipass welding process with distributed heat source. *J. Braz. Soc. Mech. Sci. Eng.* 25(3), 302-305.
[32] Nguyen N.T., Mai Y.W., Simpson S., Ohta A. (2004). Analytical approximate solution for double ellipsoidal heat source in finite thick plate. *Welding J.* 83, 82s-93s.
[33] Kang S.H., Cho H.S. (1999). Analytical solution for transient temperature distribution in gas tungsten arc welding with consideration of filler wire. *Proc. Inst. Mech. Engrs.* 213B, 799-811.
[34] Myśliwiec M. (1970). *Thermo-mechanical fundamentals of welding*. WN-T, Warszawa 1970 (in Polish).
[35] Radaj D. (1992). *Heat effects of welding. Temperature field, residual stress, distortion*. Springer-Verlag, Berlin Heidelberg, New York, London, Paris, Tokyo.
[36] Easterling K.E. (1993). Modelling the weld thermal cycle and transformation behaviour in the hest affected zone. In: H.K.E. Cerjak, K.E. Easterling (Eds), *Mathematical modelling of weld phenomena*, The Institute of Materials, London.
[37] Winczek J. (2008). Modelling of HAZ in rectangular prismatic steel casts regenerated by weave bead up. *Arch. Foundry Eng.* 8 (Special Issue 1), 331-336.
[38] Winczek J. (2010). Analytical solution to transient temperature field in a half-infinite body caused by moving volumetric heat source, *Int. J. Heat Mass Transfer* 53, 5774-5781.
[39] Vishnu P.R., Li W.B., Easterling K.E. (1991). Heat-flow model for pulsed welding. *Mater. Sci. Technol.* 7, 649-659.
[40] Modenesi P.J., Reis R.I. (2007). A model for melting rate phenomena in GMA welding. *J. Mater. Proc. Technol.* 189, 199–205.
[41] Hrabe P., Choteborsky R., Navratilova M. (2009). Influence of welding parameters on geometry of weld deposit bead, In Int. Conf. Economic Eng. Manufacturing Systems, Brasov, 26 – 27 November 2009, Regent 10 3(27) 291-294.
[42] Klimpel A., Balcer M., Klimpel A.S., Rzeźnikiewicz A. (2006). The effect of the metod and parameters in the GMA surfacing with solid wires on the quality of pudding welds and the content of the base material in the overlay. *Welding Int.* 20(11), 845-850.